Teaching cases in nuclear oncology

Lorenzoni, Alice; Alessi, Alessandra; Crippa, Flavio; Shammari, S.; Fraioli, F.; Telenga, E. D.; Slart, R. H.J.A.; Glaudemans, A. W.J.M.

Published in:
Nuclear Oncology

DOI:
10.1007/978-3-031-05494-5_62

Publication date:
2022

Teaching Cases in Nuclear Oncology: Breast Cancer

61

Alice Lorenzoni, Alessandra Alessi, Flavio Crippa, S. Al Shammari, F. Fraioli, E. D. Telenga, R. H. J. A. Slart, and A. W. J. M. Glaudemans

Contents

A. Lorenzoni (✉)
Nuclear Medicine Division, IRCCCS National Cancer Institute, Milan, Italy
e-mail: alice.lorenzoni@istitutotumori.mi.it

A. Alessi · F. Crippa
Nuclear Medicine and PET Unit, National Cancer Institute IRCCS, Milan, Italy

S. Al Shammari · F. Fraioli
Institute of Nuclear Medicine, UCLH NHS Foundation Trust, London, UK

E. D. Telenga
Department of Nuclear Medicine and Molecular Imaging, University of Groningen, University Medical Center Groningen, Groningen, The Netherlands

R. H. J. A. Slart
Department of Nuclear Medicine and Molecular Imaging, University of Groningen, University Medical Center Groningen, Groningen, The Netherlands

Biomedical Photonic Imaging Group, University of Twente, Enschede, The Netherlands

A. W. J. M. Glaudemans
Biomedical Photonic Imaging Group, University of Twente, Enschede, The Netherlands

D. Volterrani et al. (eds.), *Nuclear Oncology*,
https://doi.org/10.1007/978-3-031-05494-5_62

Keywords

Breast cancer staging · [^{18}F]FDG PET/CT · Response evaluation

Abbreviations

AJCC	American Joint Committee on Cancer
CA 15-3	High-molecular weight glycoprotein, a tumor-associated marker
CEA	Carcinoembryonic antigen, a tumor-associated marker
CT	X-ray computed tomography
ER	Estrogen receptor
[^{18}F] FDG	2-Deoxy-2-[^{18}F]fluoro-D-glucose
^{18}F-FES	16α-^{18}F-Fluoro-17β-estradiol
^{18}F-FLT	^{18}F-3′-deoxy-3′-fluorothymidine
HER2/neu	Human epidermal growth factor receptor 2
M	Metastasis status according to the AJCC/UICC TNM staging system
MIP	Maximum intensity projection
N	Lymph node status according to the AJCC/UICC TNM staging system
PET	Positron emission tomography
PET/CT	Positron emission tomography/Computed tomography
PR	Progesterone receptor
SUV	Standardized uptake value
SUV_{max}	Standardized uptake value at point of maximum
T	Tumor status according to the AJCC/UICC staging system
^{99m}Tc-HDP	^{99m}Tc-hydroxyethylene-diphosphonate
TNBC	Triple negative breast cancer
UICC	Union Internationale Contre le Cancer (International Union Against Cancer)

Case No. 1

Presentation

A 76-year-old woman with a recent diagnosis of invasive ductal carcinoma of the left breast (6 cm in size) and suspected left axillary lymph node involvement was referred for [^{18}F]FDG PET/CT for staging.

Findings

PET/CT imaging showed the presence of an [^{18}F]FDG-avid mass in central and lower quadrants of the left breast corresponding to the diagnosed carcinoma. Bilateral axillary lymph nodes with high [^{18}F]FDG uptake suspicious for node involvement were also noted. Furthermore, there were multiple foci of [^{18}F]FDG uptake in dorsal and lumbar spine, consistent with bone metastases (Figs. 1, 2, and 3).

Discussion

[^{18}F]FDG PET/CT is an important imaging modality for the detection of locoregional and metastatic spread in the appropriate patient population; while [^{18}F]FDG PET should not be used routinely for initial detection of breast cancer or for detection of axillary nodal involvement, [^{18}F]FDG PET in higher-risk populations has great value in definitive whole body initial staging.

Case No. 2

Presentation

A 58-year-old woman presented with mammographic evidence of tissue distortion and microcalcification of the upper outer quadrant of left breast. Core biopsy showed invasive lobular carcinoma, ER-positive, PR-positive, and negative for human epidermal growth factor receptor 2 (HER2/neu). [^{18}F]FDG PET/CT was performed to complete staging before planned surgery.

Findings

[^{18}F]FDG PET/CT did not show foci of suspected tracer uptake in the upper outer quadrant of the left

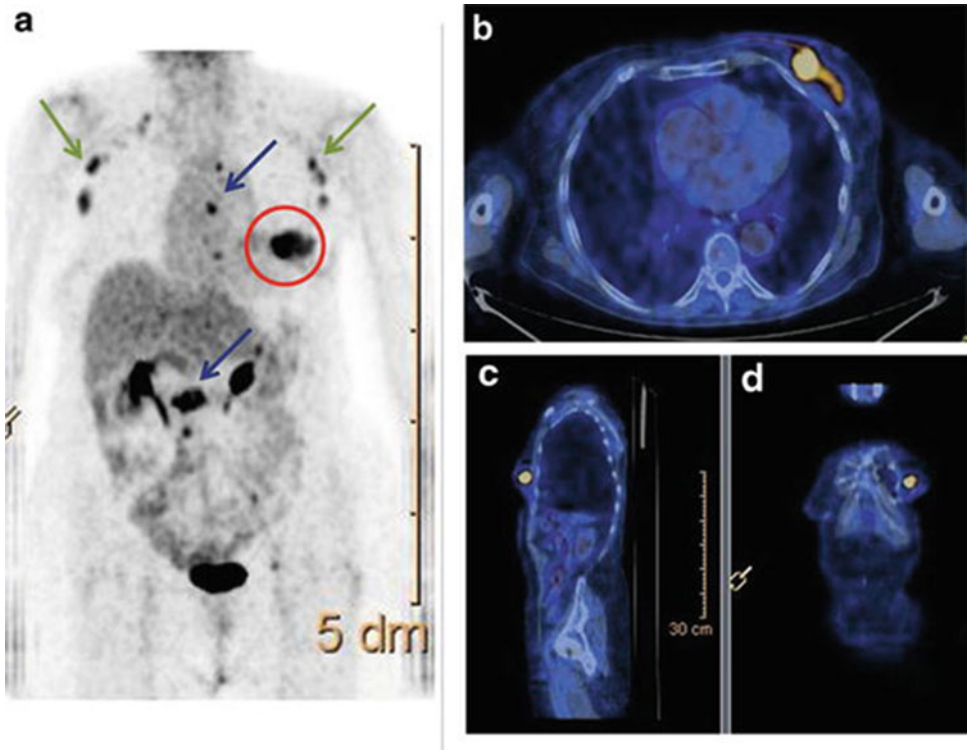

Fig. 1 Maximum intensity projection (*MIP*) (**a**, red circle), axial (**b**), sagittal (**c**), and coronal fused PET/CT images of the [^{18}F]FDG-avid left breast lesion. The MIP image clearly demonstrated bilateral axillary lymph node involvement (green arrows) and bone metastases (blue arrows)

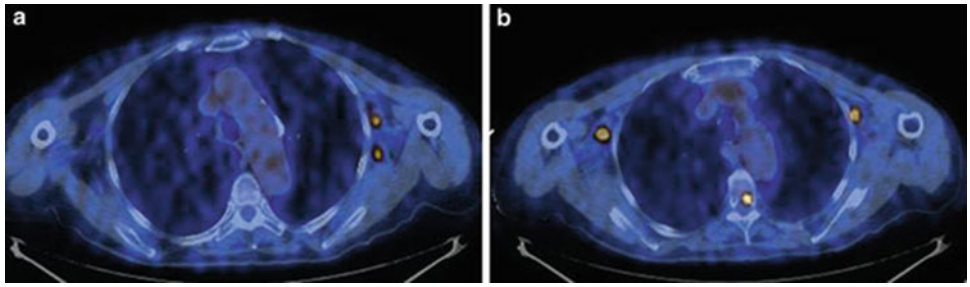

Fig. 2 Axial fused image of axillary hypermetabolic lymph nodes and focal uptake of dorsal spine consistent with skeletal metastasis

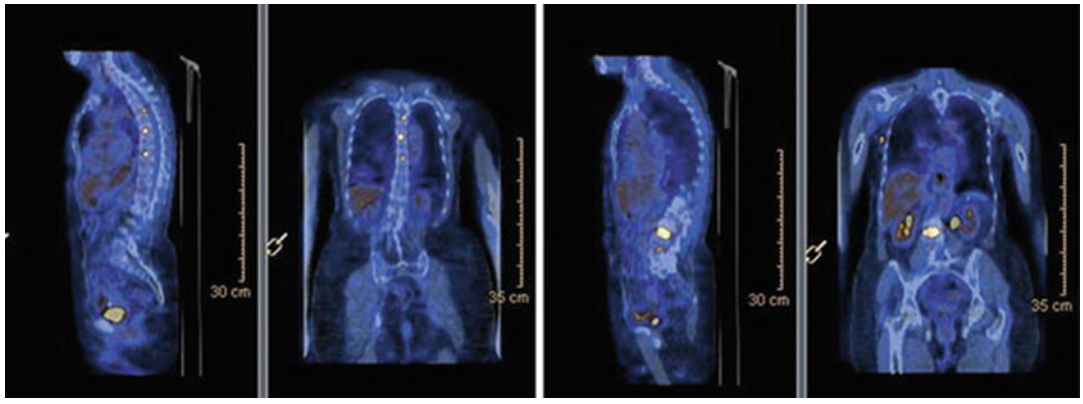

Fig. 3 Fused coronal and sagittal PET/CT images showing metastatic bone involvement of dorsal (left panel) and lumbar (right panel) spine

breast (Fig. 4). Whole body staging was negative for detection of axillary involvement and distant metastasis. Breast-conserving surgery consistent with quadrantectomy and sentinel lymph node biopsy were performed. Histology showed micrometastasis in the sentinel lymph node.

Discussion

The ability of PET to detect breast cancer depends on the tumor's size and histology (e.g., low [^{18}F]FDG avidity in grade 1 cancer and/or in lobular carcinoma). Sensitivity of [^{18}F]FDG PET has been reported to be 68% for small (<2 cm) tumors and 92% for larger (2–5 cm) tumors, and its reported overall accuracy for detecting in situ carcinomas is low (sensitivity, 2–25%).

There is also a correlation between the tumor proliferation index (Ki67 expression) and the intensity of [^{18}F]FDG uptake. [^{18}F]FDG PET has moderate accuracy for detecting axillary metastasis, as it often fails to detect early axillary node involvement and micrometastases.

Case No. 3

Presentation

A 42-year-old lady with a recent diagnosis of breast cancer was referred for [^{18}F]FDG PET/CT for staging.

Findings

There was an [^{18}F]FDG-avid lesion in right breast (measuring ~1.4 × 1 cm, SU_{max} 7, long arrow in upper, axial PET/CT image). There was also a

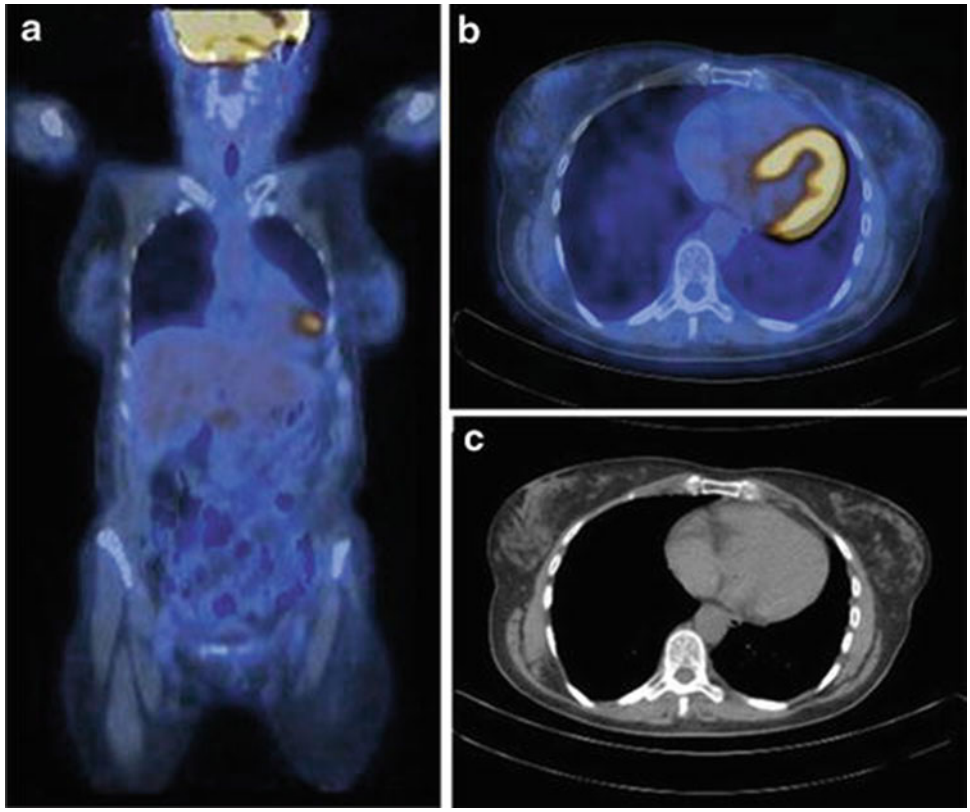

Fig. 4 Fused coronal [^{18}F]FDG PET/CT (**a**) and axial images ((**b**) fused PET/CT and (**c**) low-dose CT) failed to detect the malignant left breast lesion

mildly [^{18}F]FDG-avid level III right axillary lymph node (measuring ~7 mm, with SUV_{max} 2.0, short arrow). Histopathology of the right axillary lymph node confirmed the diagnosis of nodal involvement.

Discussion

The ability of [^{18}F]FDG PET to detect breast cancer depends on the tumor's size and histology. The sensitivity of PET has been reported to be 68% for small (<2 cm) tumors and 92% for larger (2–5 cm) tumors. Overall accuracy for detecting in situ carcinomas is low (25% sensitivity at most). The major limitation of PET or PET/CT for breast imaging is its poor detection rate for small breast carcinomas and noninvasive breast cancers. However, PET/CT has a role to play in a group of patients, such as those with dense breasts or with implants, for determining tumor multiplicity, for localizing the primary tumor in those patients with metastasis of breast origin when the mammography is indeterminate, and for those patients where biopsy is not a desirable option. Regional lymph node assessment of the axilla, internal mammary, or mediastinum is an important factor to assess the prognosis of patients with breast cancer. PET/CT can be a valid option to localize and differentiate metastatic and reactive lymph nodes when CT shows multiple enlarged lymph nodes in the axilla. Distant metastases from breast cancer are frequently found in the lungs, liver, and bones. One advantage of whole body PET imaging over conventional imaging modalities is its ability to detect metastasis at different sites and organs during a single examination.

Case No. 4

Presentation

A 38-year-old woman with recent diagnosis of locally advanced triple-negative breast cancer (TNBC) underwent [^{18}F]FDG PET for staging before scheduled chemotherapy.

Findings

[^{18}F]FDG-avid multiple left breast lesions were noted. Enlarged left axillary lymph nodes with pathological [^{18}F]FDG uptake were also observed (Fig. 5). Furthermore, a previously unknown [^{18}F]FDG-avid lymph node was clearly depicted in the ipsilateral subclavicular region (Fig. 5). The patient underwent anthracycline-based regimen. After chemotherapy completion, [^{18}F]FDG PET/CT was performed to evaluate response to treatment. Whole body PET/CT did not show pathological radiopharmaceutical uptake, consistent with complete metabolic response (Fig. 6).

Discussion

Triple negative breast cancer is an aggressive heterogeneous group of tumors, constituting 15% of invasive breast tumors. The majority of TNBCs are aggressive basal-like subtypes presenting with larger tumors of higher grade and increased numbers of involved nodes. Patients with TNBC have a relatively poor outcome; however, this tumor has more intrinsic responsiveness to chemotherapy than estrogen receptor-positive tumors. Stratification of TNBC prognosis would be highly desired, since some patients with better prognosis might benefit from appropriate targeted treatment.

TNBC tumors typically have higher metabolic activities (expressed as [^{18}F]FDG uptake) of than those of other phenotype breast cancers. Pretreatment [^{18}F]FDG PET/CT imaging may have a significant prognostic value for predicting survival outcome of TNBC patients. Furthermore, [^{18}F]FDG PET/CT after two cycles of neoadjuvant chemotherapy may identify poor metabolic responders, who have a high risk of early relapse.

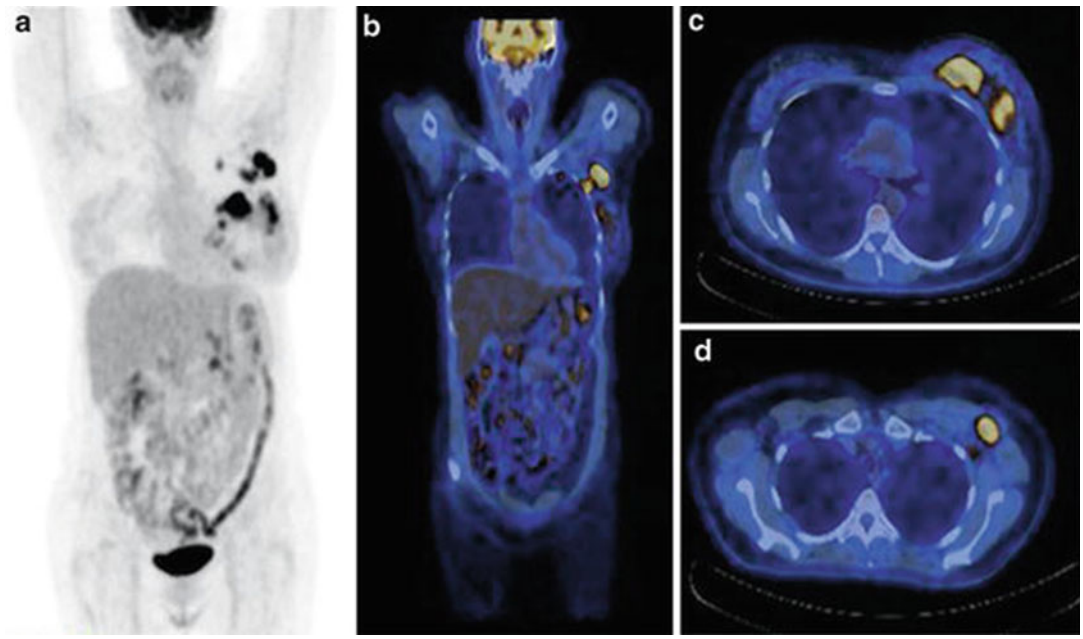

Fig. 5 Baseline whole body [^{18}F]FDG PET/CT in patient with locally advanced TNBC (**a**, maximum intensity projection). Fused PET/CT images show multifocal [^{18}F]FDG-avid primary breast tumor (**b**, **c**), pathological hypermetabolic lymph nodes in the left axillary (**b**, **d**) and in the ipsilateral subclavicular regions (**b**)

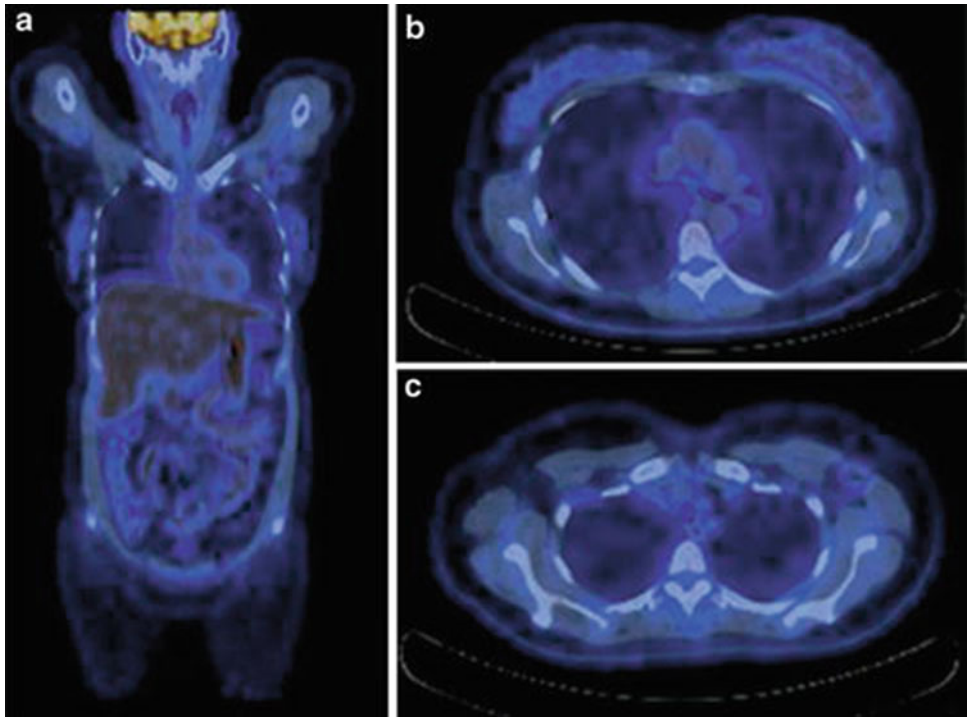

Fig. 6 Fused PET/CT images ((**a**) coronal, (**b**, **c**) transaxial) after chemotherapy completion show the disappearance of the previously detected pathological [^{18}F]FDG uptake in left breast and in regional lymph nodes

Case No. 5

Presentation

A 38-year-old woman who previously received neoadjuvant chemotherapy and curative resection of a right breast cancer was referred for sudden-onset chest pain lasting for 15 days. Right pleural effusion was demonstrated. Thoracentesis was performed and pleural fluid analysis showed light yellow and clear fluid with no evidence of malignancy. High values of CA 15-3 and CEA were present (65.6 U/mL and 18 ng/mL, respectively). [^{18}F]FDG PET/CT was performed for suspected recurrent breast cancer to evaluate the presence of disease.

Findings

[^{18}F]FDG PET/CT images (Figs. 7 and 8) showed diffuse intense [^{18}F]FDG uptake of the right pleura suspicious for metastatic disease. Marked focal increased metabolic activity in segment 7 of the liver was also demonstrated, consistent with hepatic metastasis. Furthermore, [^{18}F]FDG-avid abdominal para-aortic lymph node and sternal lesion were depicted. PET/CT findings clearly demonstrated stage IV recurrent breast cancer.

Discussion

Approximately 30–50% of breast cancer patients have a recurrence of disease within 10 years after diagnosis. The [^{18}F]FDG PET/CT scan plays an important role in restaging breast cancer patients with rising tumor markers and negative or equivocal findings on conventional imaging techniques, with high sensitivity (>90%) and a change in planned therapy in about 50% of the cases.

[^{18}F]FDG PET allows more accurate diagnosis of metastatic disease in patients with treated breast cancer and patients with rising levels of tumor

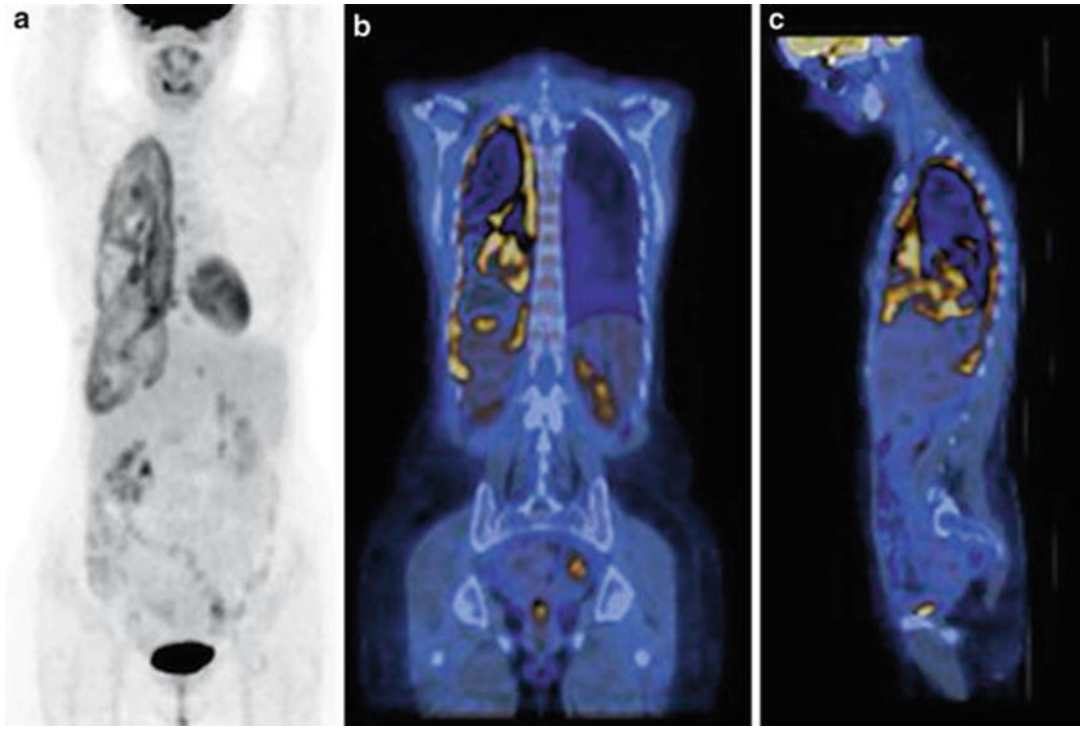

Fig. 7 Whole body [^{18}F]FDG PET/CT in patient with suspected recurrent breast cancer ((**a**), maximum intensity projection, (**b**) coronal fused PET/CT, (**c**) sagittal fused PET/CT). Diffuse intense [^{18}F]FDG uptake of the right pleura suspicious for metastatic disease is shown. Right pleura effusion without significant metabolic activity

markers compared with CT alone demonstrating improved sensitivity, specificity, accuracy, and predictive value.

Case No. 6

Presentation

A 28-year-old woman referred for [^{18}F]FDG PET/CT for staging with diagnosis of right breast cancer cT1N1 (CDI, G2, ER = 95%, PR = 95%, HER2 = ISH not amplified, Ki-67 = 80%) and synchronous skeletal metastases, for treatment planning.

Findings

A baseline [^{18}F]FDG PET/CT was performed prior to chemotherapy. PET/CT images demonstrated a small [^{18}F]FDG-avid nodule in the upper inner quadrant of the right breast, corresponding to the known malignancy (Fig. 9). Focal increased [^{18}F]FDG activity was noted in the right humerus, spine, pelvic skeleton, and femora (Fig. 9).

After chemotherapy, [^{18}F]FDG PET/CT was performed to evaluate response to treatment. The PET/CT images showed metabolic progression of the right mammary nodule (Fig. 10) and of bone disease (Fig. 11).

Discussion

Treatment of breast cancer patients who have metastatic disease aims to improve survival and quality of life, since the disease is generally not curable. It is therefore essential to identify patients who do not respond to chemotherapy, in order to avoid ineffective therapies and unnecessary side effects.

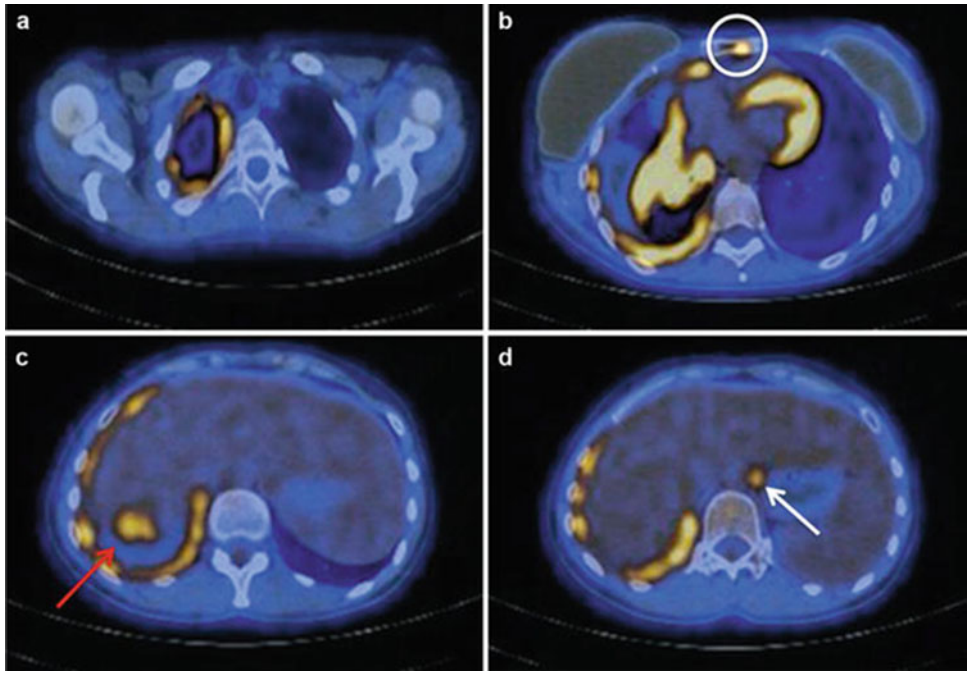

Fig. 8 Fused transaxial PET/CT images show pathological pleural [^{18}F]FDG uptake (**a**– **d**), sternal [^{18}F]FDG-avid lesion (**b**, white circle), liver metastasis (**c**, red arrow), and abdominal lymph node involvement (**d**, white arrow) consistent with distant metastatic recurrence of breast cancer

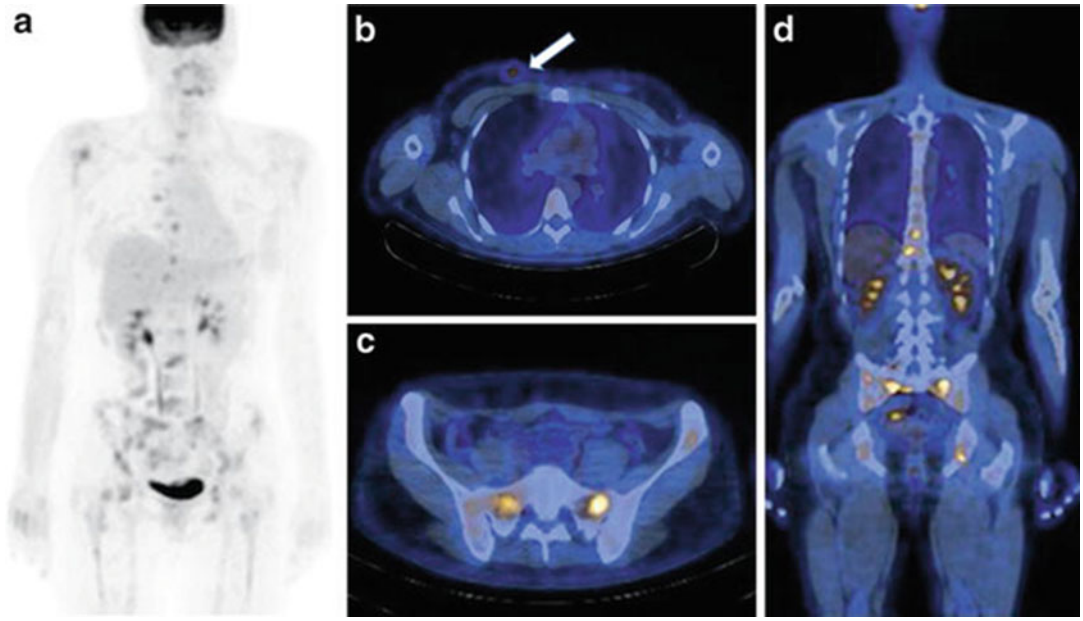

Fig. 9 Baseline [^{18}F]FDG PET/CT in patient with right breast cancer and metastatic bone lesions (**a**, MIP). Axial fused PET/CT image of [^{18}F]FDG-avid breast nodule (**b**, white arrow). Diffuse bone involvement consistent with multiple focal increased metabolic activity was revealed (**a**, **c**, and **d** images)

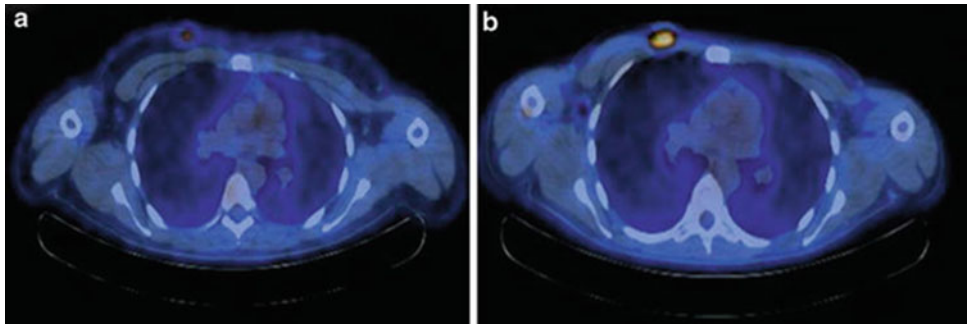

Fig. 10 Fused transaxial images of [^{18}F]FDG PET/CT performed to evaluate treatment response show metabolic and dimensional progression of primary tumor (**a** before therapy, **b** after therapy completion)

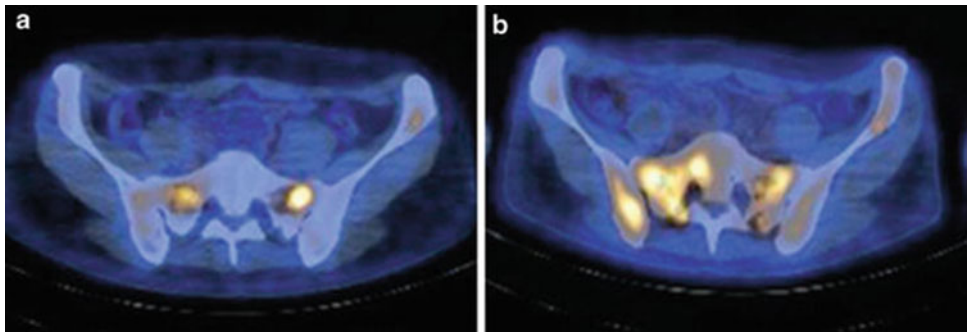

Fig. 11 Bone disease progression after chemotherapy demonstrated by fused [^{18}F]FDG PET/CT images (**a** at baseline, **b** after therapy)

Changes in tumor metabolic activity have been shown to be an important indicator of treatment effectiveness for breast cancer. In patients with metastatic breast cancer, the effectiveness of chemotherapy can be evaluated earlier with [^{18}F]FDG PET than with conventional imaging. Another important finding is that PET/CT allows evaluation of response in many different metastases. Therefore, PET/CT is helpful to detect a heterogeneous response (coexistence of responding and nonresponding lesions within the same patient). Furthermore, metastatic bone lesions, the most common site of breast cancer metastases, occurring in up to 80% of patients, are often difficult to assess for response by conventional imaging such as CT and bone scans. In this setting, [^{18}F]FDG PET/CT may play an important role in assessing response to therapy in bone-dominant breast cancer (Figs. 12 and 13) [1–3].

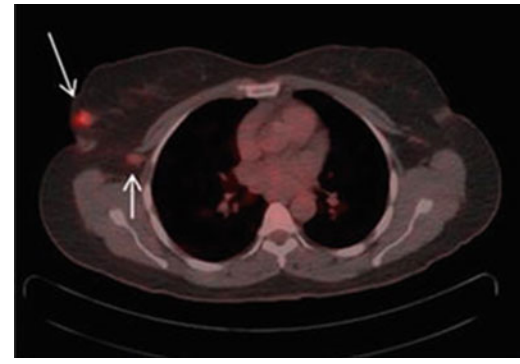

Fig. 12 Fused PET/CT transaxial image of [^{18}F]FDG-avid right breast lesion and ipsilateral axillary lymph node

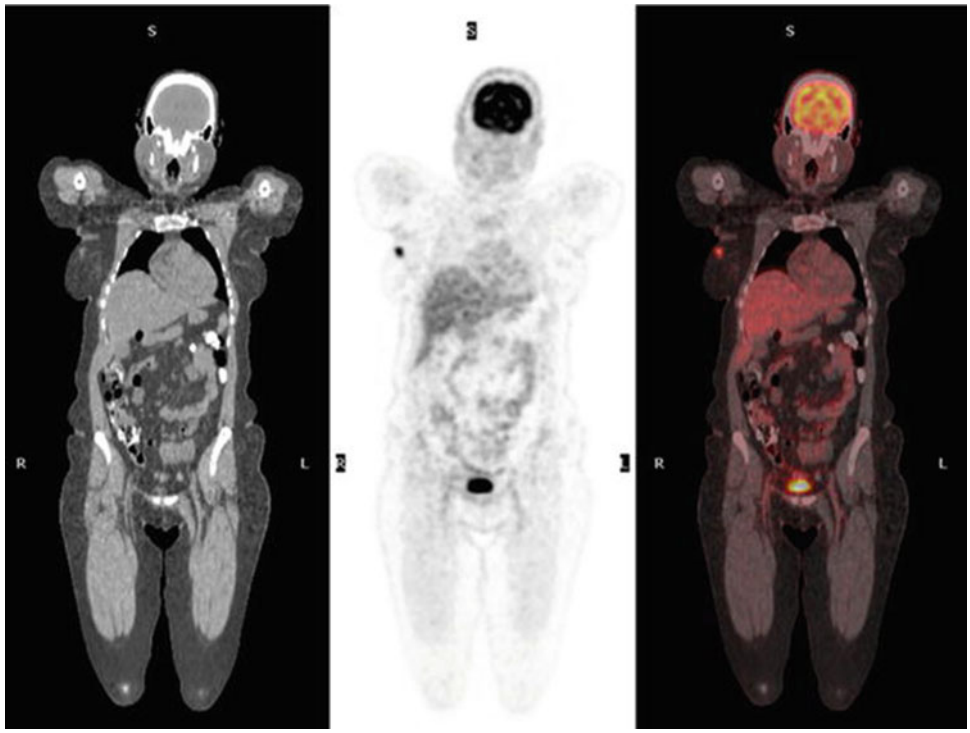

Fig. 13 Coronal image of right breast lesion

Case No. 7

Presentation

A 72-year-old woman had been treated 13 years earlier with left-sided mastectomy and axillary lymph node dissection for an ER-positive, PR-negative breast carcinoma. Now, she presents with a lesion in the postmastectomy scar. Biopsy showed an infiltrative lobular carcinoma, ER-positive, PR-positive, and Her2/neu-negative.

Findings

^{99m}Tc-HDP bone scintigraphy showed a small lesion in the right frontal bone as the only possible bone metastasis (Fig. 14), although a solitary bone island or hyperostosis frontalis was also considered for differential diagnosis. Because of the uncertainty about the possible solitary metastasis, the patient was accepted for curative treatment and the lesion in the left breast region was resected. Pathology showed an infiltrative lobular carcinoma (2.2 cm in maximum diameter), with residual focal tumor growth at 1 mm from the resection margin. Additional imaging was therefore performed before possible treatment with radiotherapy and hyperthermia.

[^{18}F]FDG PET/CT showed increased uptake at the left thoracic wall, consistent with inflammation due to recent surgery (Fig. 15). Furthermore, there was a small moderately intense lesion on the left side of first lumbar vertebra (SUV_{max} 4.0). On the low-dose CT, multiple sclerotic lesions not associated with increased [^{18}F]FDG uptake were seen in the frontal bone, the spine, and pelvis.

To further characterize these sclerotic lesions, the patient was referred for a PET/CT scan with ^{18}F-FES, which was performed 1 month after the

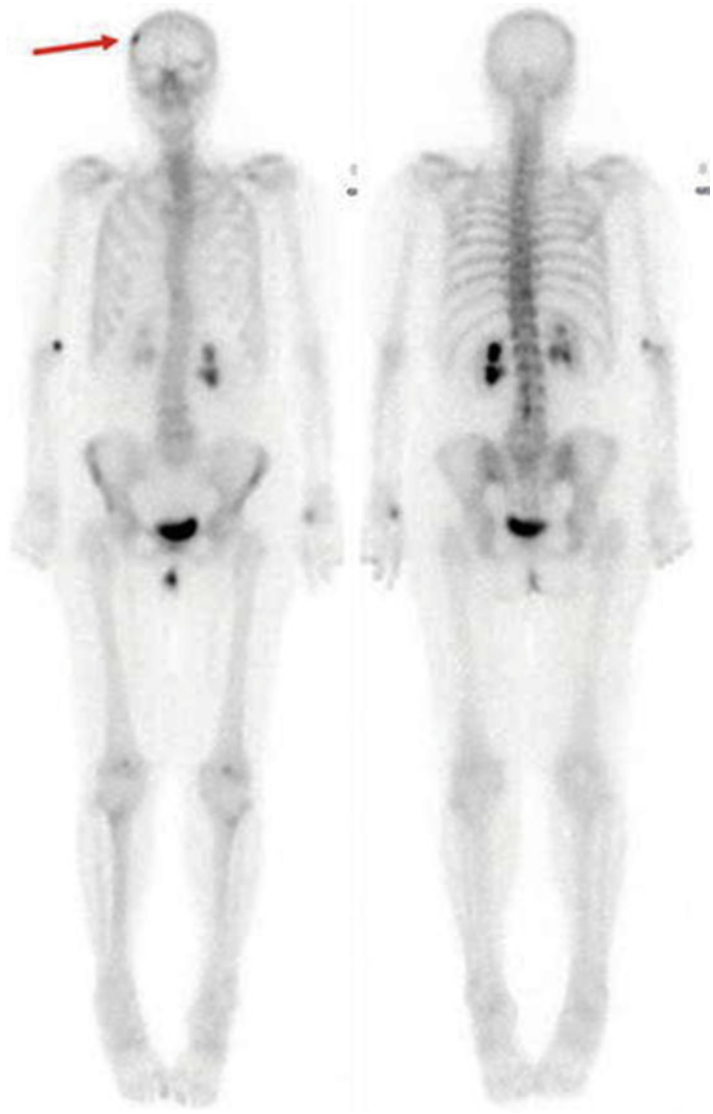

Fig. 14 Anterior (left panel) and posterior (right panel) ^{99m}Tc-HDP bone scintigraphy showing a solitary lesion in the right frontal bone (red arrow)

[^{18}F]FDG PET/CT scan. ^{18}F-FES PET/CT showed multiple lesions with increased uptake throughout the skeleton, as well as multiple ^{18}F-FES-avid axillary, mediastinal, lung hilar, and paraaortic abdominal lymph nodes (Fig. 15). The lesion seen in the first lumbar vertebra on the [^{18}F]FDG PET/CT scan also showed moderately intense uptake of ^{18}F-FES; however, the ^{18}F-FES PET/CT scan showed two additional lesions with intense ^{18}F-FES uptake

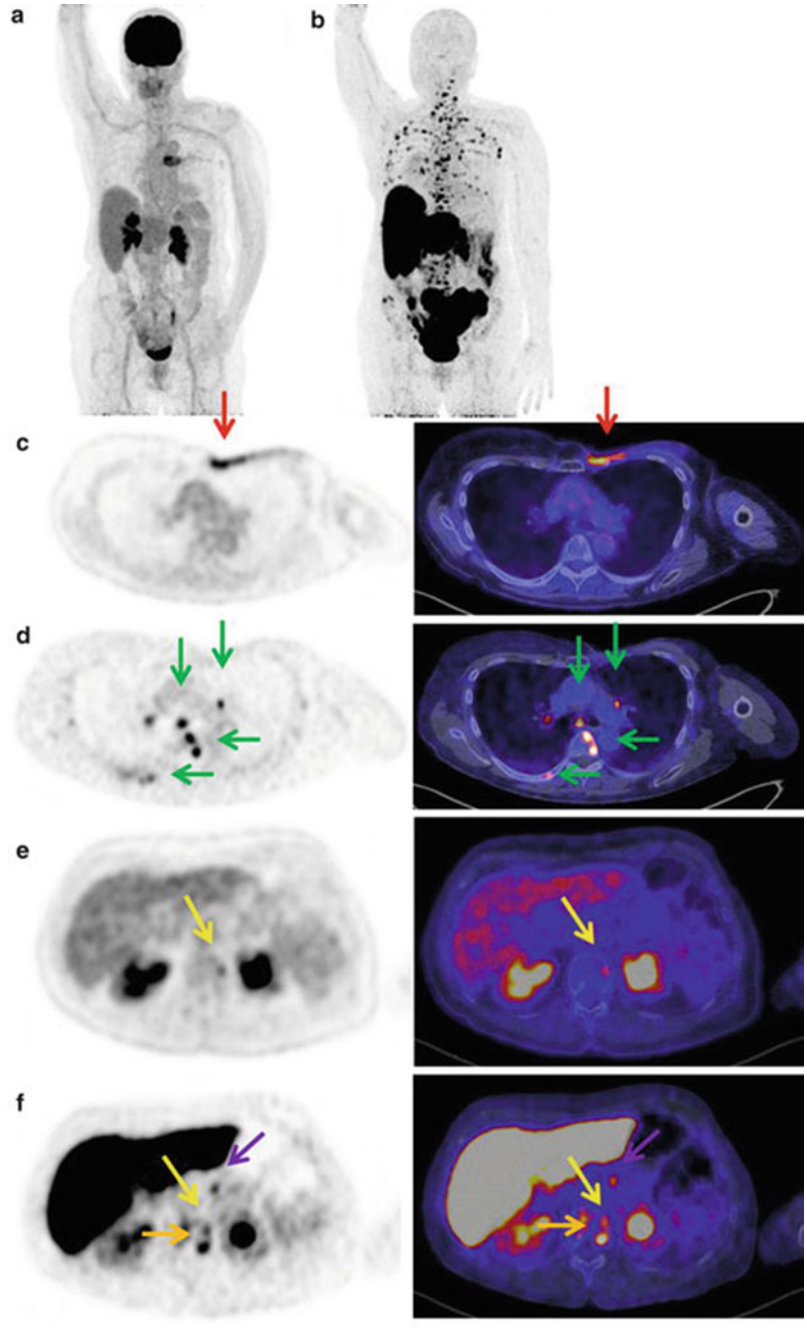

Fig. 15 [^{8}F]FDG PET/CT (left side: **a**, **c**, and **e**) and ^{18}F-FES PET/CT (right side: **b**, **d**, and **f**); **a** and **b** are MIP images. **c**, **d**: increased [^{18}F]FDG uptake and no ^{18}F-FES uptake at the left thoracic wall (red arrows); however, there is increased ^{18}F-FES uptake in the vertebra, rib, subcarinal, and lung hilar lymph nodes (green arrows). **e**, **f**: moderately increased [^{18}F]FDG and ^{18}F-FES uptake in a lesion in the left portion of L1 (yellow arrows). More intense ^{18}F-FES uptake in two additional lesions in the same vertebra without [^{18}F]FDG uptake (orange arrows). Increased ^{18}F-FES uptake in a left para-aortic lymph node (purple arrows)

in the same vertebral body that were not visible at all on the [^{18}F]FDG PET/CT (Fig. 15e, f). The sclerotic lesion in the frontal bone was negative on both scans.

Follow-Up

Based on the ^{18}F-FES PET/CT findings, it was concluded that the patient had extensively metastatic

breast cancer. Therapy with aromatase inhibiting drugs was therefore started and the patient was referred for further palliative care.

Case No. 8

Presentation

A 42-year-old woman referred with diagnosis of infiltrating ductal carcinoma with squamous differentiation of the left breast (cT2N1).

Findings

^{18}F-3′-deoxy-3′-fluorothymidine (^{18}F-FLT) PET/CT performed before neoadjuvant chemotherapy demonstrated a focal increased of tracer uptake in the upper-outer quadrant of left breast consistent with known malignancy. Furthermore, there was a mildly ^{18}F-FLT-avid left axillary lymph node (Fig. 16).

After chemotherapy, ^{18}F-FLT PET/CT performed to evaluate treatment response showed reduction of the focal increased ^{18}F-FLT activity in left breast and the disappearance

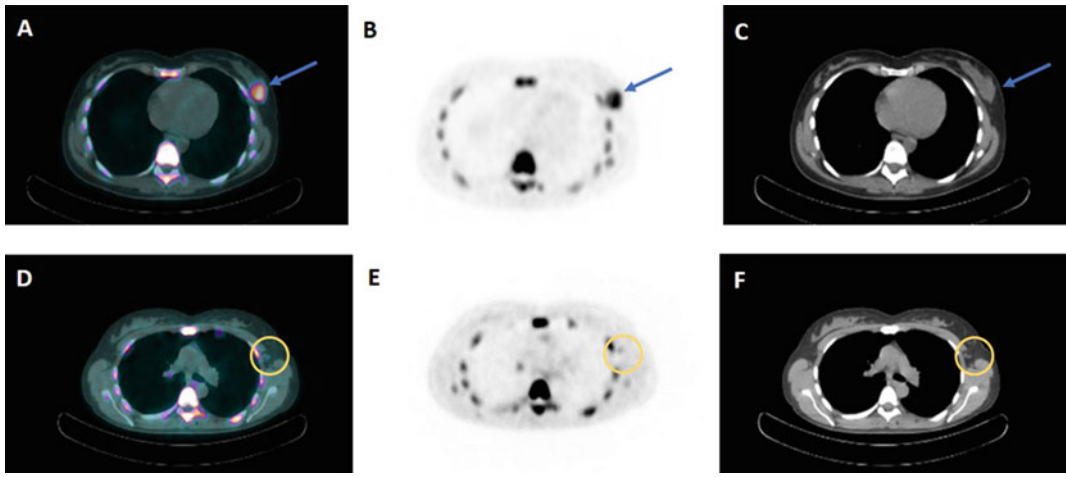

Fig. 16 ^{18}F-FLT PET/CT of left breast lesion (upper row, blue arrow; **a** transaxial fused PET/CT; **b** transaxial PET; **c**, transaxial CT) and ipsilateral axillary lymph node (bottom, yellow circle; **d** transaxial fused PET/CT; **e** transaxial PET; **f**, transaxial CT)

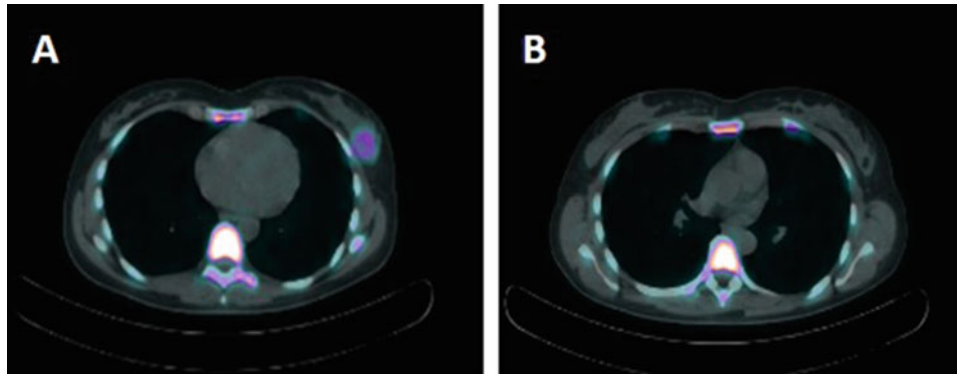

Fig. 17 ^{18}F-FLT PET/CT after chemotherapy completion, showing reduction of pathological ^{18}F-FLT activity in left breast lesion (**a**, transaxial fused PET/CT) and disappearance of tracer uptake in ipsilateral axillary lymph node (**b**, transaxial fused PET/CT)

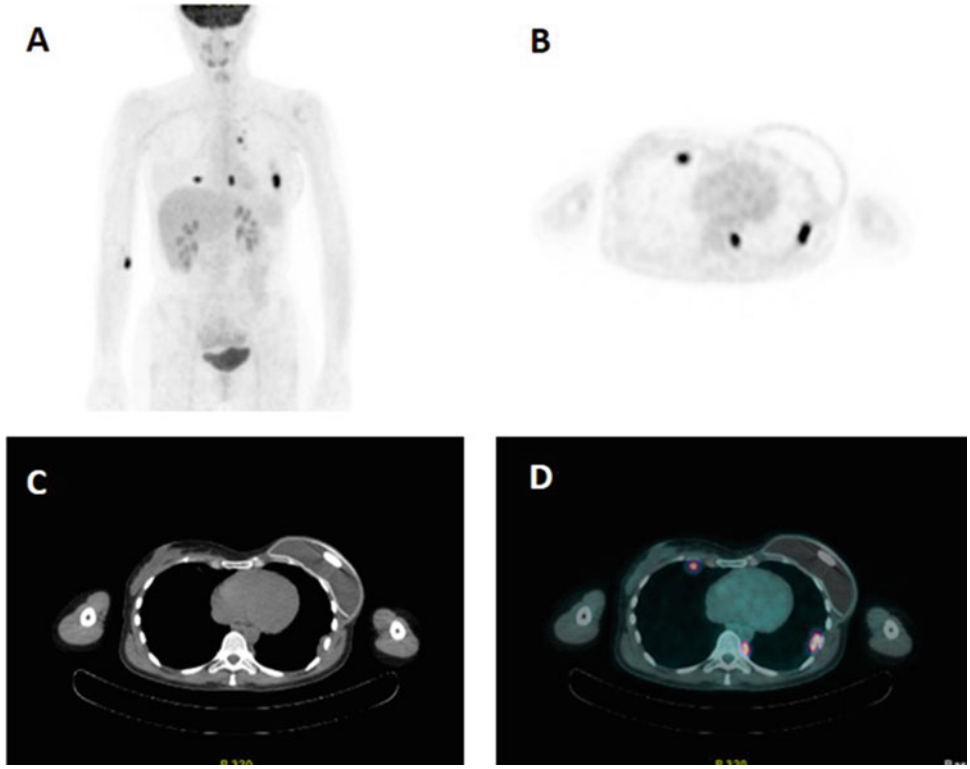

Fig. 18 [^{18}F]FDG PET/CT of nodular pleural thickenings (**a**, MIP; **b**, transaxial PET; **c**, transaxial CT; **d**, transaxial fused PET/CT)

of pathological uptake in ipsilateral axillary lymph node (Fig. 17).

Mastectomy and concomitant sentinel lymph node biopsy were performed, with diagnosis of pT2N0 CDI, G3 ER-, PgR-, HER2 0, Ki67 92%. Follow-up [^{18}F]FDG PET/CT performed 1 year later showed the appearance of hypermetabolic nodular pleural thickenings consistent with metastases (Fig. 18).

Discussion

^{18}F-FLT has been shown to be helpful as a potential indicator of tumor response or resistance to therapy in breast cancer. In fact, ^{18}F-FLT uptake reflects activity of the enzyme thymidine kinase-1 (TK1), well known for its function in the pyrimidine salvage pathway. This enzyme is upregulated during the late G1/S phase of the cell cycle, thus representing an indirect marker of cell proliferation.

References

1. Yue Y, Cui X, Bose S, et al. Stratifying triple-negative breast cancer prognosis using ^{18}F-FDG-PET/CT imaging. Breast Cancer Res Treat. 2015;153:607–16.
2. Groheux D, Biard L, Giacchetti S, et al. ^{18}F-FDG PET/CT for the early evaluation of response to neoadjuvant treatment in triple-negative breast cancer: influence of the chemotherapy regimen. J Nucl Med. 2016;57:536–543.
3. Groheux D, Hindié E, Giacchetti S, et al. Early assessment with ^{18}F-fluorodeoxyglucose positron emission tomography/computed tomography can help predict the outcome of neoadjuvant chemotherapy in triple negative breast cancer. Eur J Cancer. 2014;50:1864–71.